Geodata Science Presentations
Department of Earth, Atmospheric, and Planetary Sciences

12-9-2019

Crustal Structure from Correlation Analysis of the Coda of Local Seismicity Beneath a Large-N Array

Qicheng Zeng

Robert L. Nowack

Crustal Structure from Correlation Analysis of the Coda of Local Seismicity Beneath a Large-N Array

Qicheng Zeng[1] (zeng181@purdue.edu) and Robert L. Nowack[1]
[1]Dept of Earth, Atmos. and Planetary Sciences, Purdue University, West Lafayette, IN, USA

ABSTRACT

The seismic coda from frequent local seismicity near the large-N IRIS Community Wavefield Experiment in Oklahoma was used to estimate crustal structure beneath the array. Because of the number of these events, their coda make up a component of the local noise-field and also have predominantly body-wave components as recorded by the array. We first identified a subset of events located beneath the array using the first arrival times of the events. Several processing methods were then applied to analyze the P-wave and S-wave coda of the events recorded by the 247 short-period nodes on the east-west and north-south lines. These methods included correlation analysis, band-pass filtering, frequency and time-domain normalization, f-k filtering and stacking. Correlation analysis was used to eliminate the effects of the event depth and redatum the events to virtual source locations. The correlation results recovered seismic reflections from Moho and several crustal interfaces with high reflectivity. Ray tracing was then applied to convert travel-times to depth based on the velocity models of OGS and Crust 1.0 for the area. The recovery of crustal structure from the correlation analysis of local P-wave and S-wave coda provides a new aspect for the usage of local seismicity beneath large-N arrays.

Map of IRIS Community Wavefield Experiment in Oklahoma

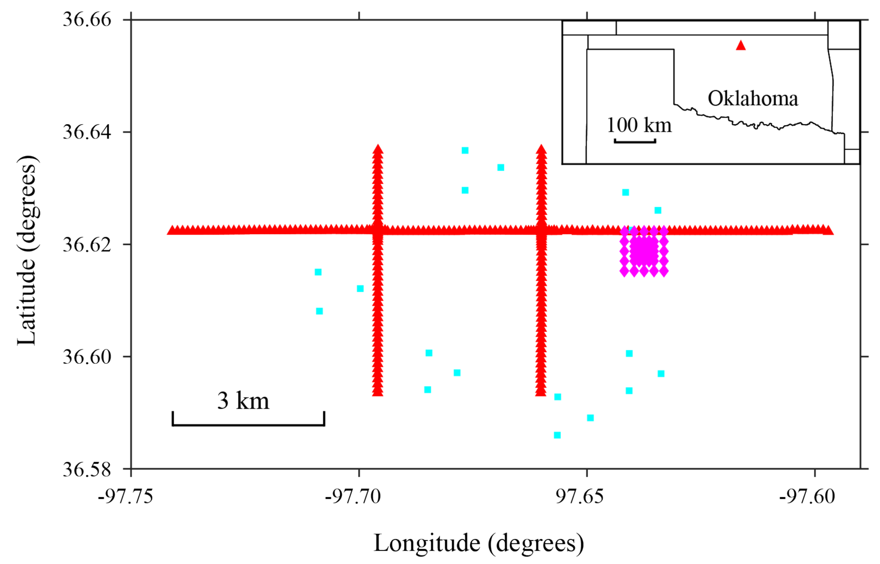

The red triangles are the north-south and east-west linear nodal array stations, the magenta diamonds denote stations from the nodal gradiometer array, and the cyan squares are the broadband stations (Sweet et al., 2018). The upper right inset map shows the location of the array by the triangle.

Seismic Events in North Central Oklahoma

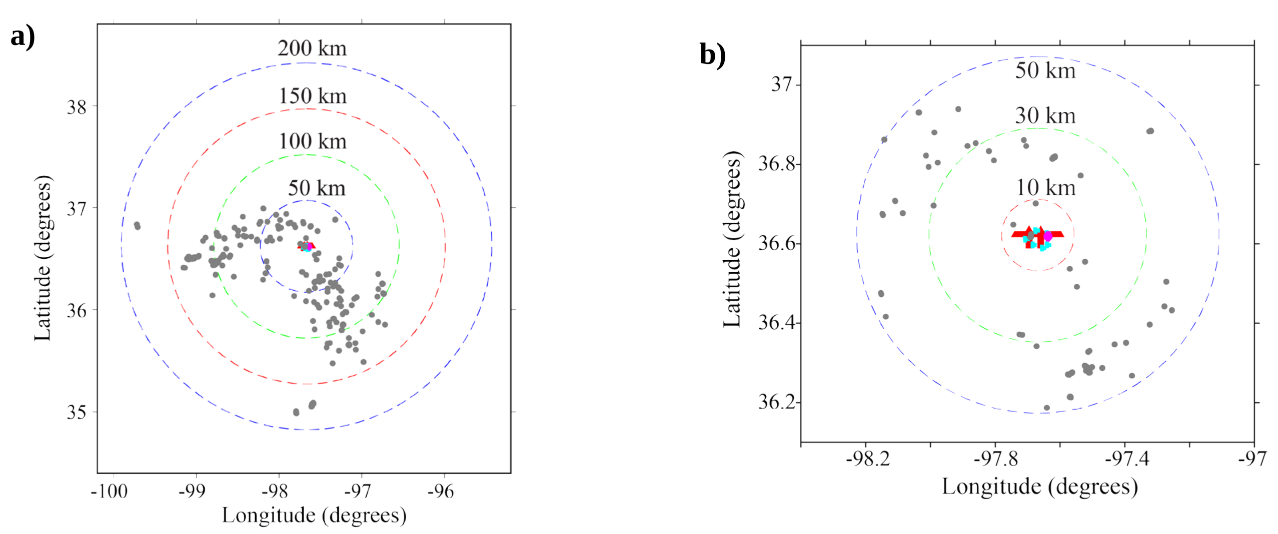

a) Map of seismic events from OGS catalog over a period from 24 June to 20 July 2016. The events are denoted by gray dots. The dashed circles have radii of 50 km, 100 km, 150 km and 200 km from the central station. b) Map of near offset events within 50 km of the central station which are used for the pre-critical data processing. The stations are denoted by red triangles, magenta diamonds and cyan squares for linear array nodes, gradiometer array and broadband stations.

Velocity Models and Predicted Arrival Time of Seismic Phases

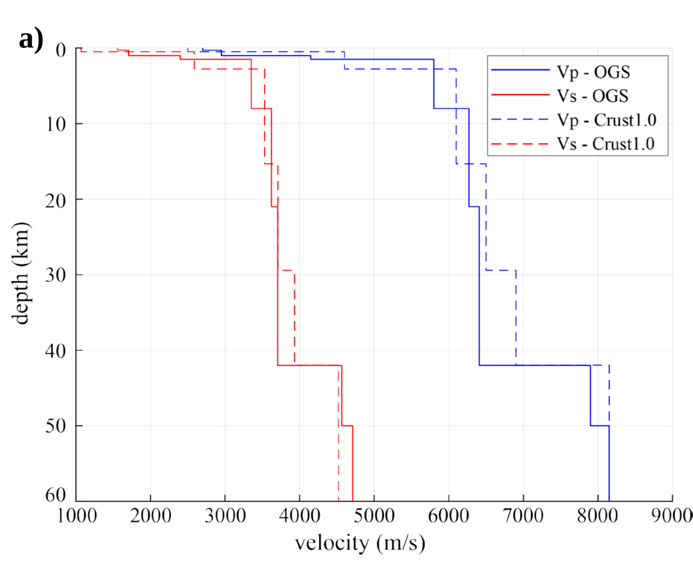

a) Velocity models of the study area. The velocity model from the Oklahoma Geological Survey (Darold et al., 2015) is denoted by solid blue and red lines. The velocity model from CRUST1.0 is shown by the dashed blue and red lines for comparison.

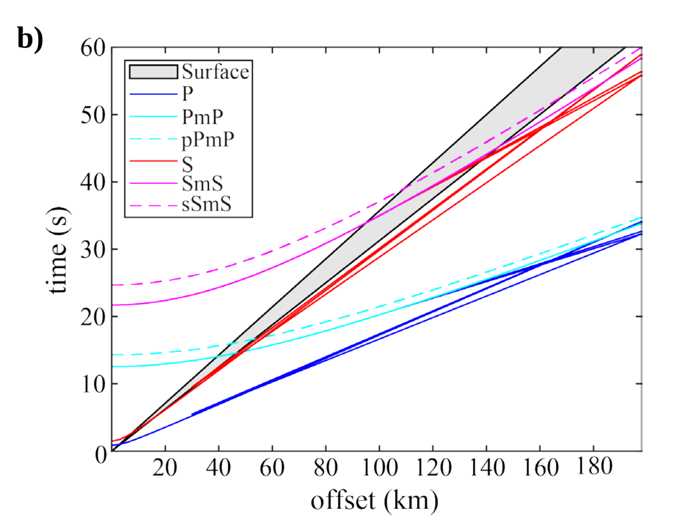

b) Travel time curves from the OGS velocity model for a 5 km focal depth source. The blue and red lines represent the direct P and S arrivals. The solid and dashed cyan lines show the downgoing and surface reflected PmP and pPmP arrivals from the Moho. The solid and dashed magenta similarly represent the SmS and sSmS arrivals. Surface wave arrivals are denoted by gray area for velocities from 2.8 km/s to 3.2 km/s.

Schematic Diagram of Normal Moveout for Events with Different Focal Depths

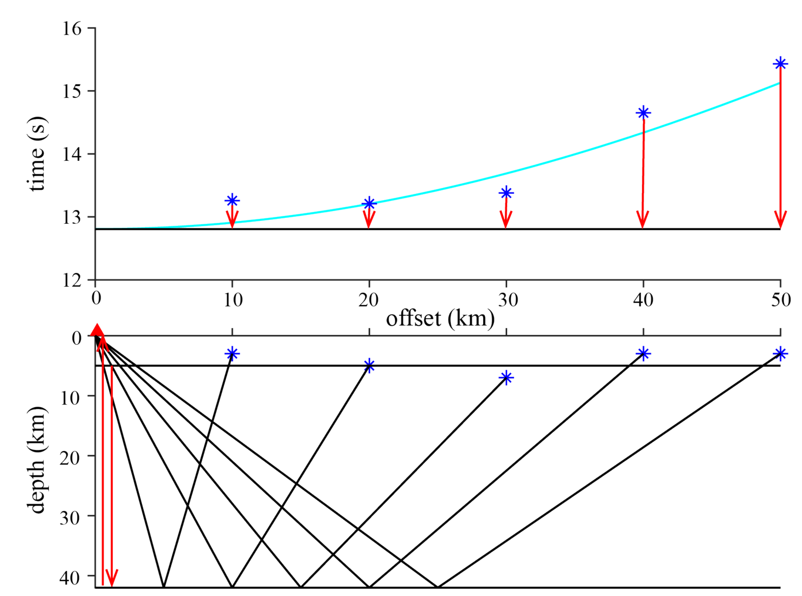

The blue asterisks represent seismic events of different offsets and focal depths from the receiver array noted by red triangle. Normal moveout is then performed on each seismic event and receiver pair. The NMO time shift flattens the arrivals and corrects for the event depths to a depth of 5 km.

Stacking for Single Event Receiver Gathers for the Vertical and Transeverse Components

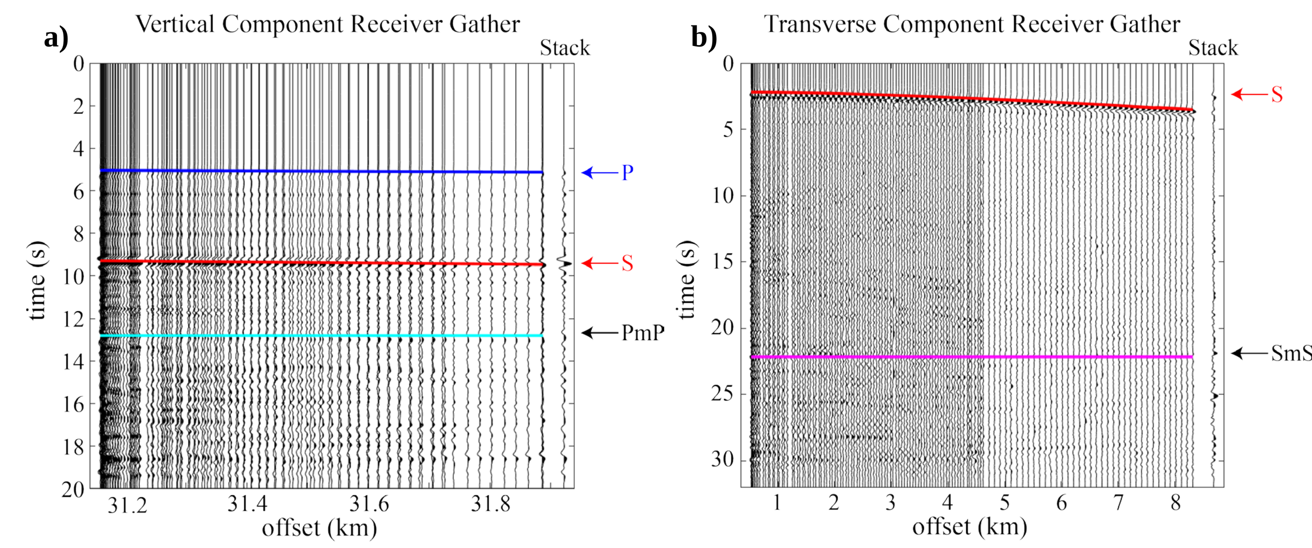

a) Single event receiver gather of the vertical component recorded by the East-West linear array nodal stations for event 25. Each trace is low-pass filtered to 2 Hz and gained by a power of t to approximately equalize the amplitudes in time. The blue, red and cyan lines are the predicted arrival times for the P, S and PmP from ray tracing, after an NMO correction for the PmP arrival. b) Single event receiver gather of the transverse component recorded by East-West linear array stations for event 2. Each trace is low-pass filtered to 1.5 Hz and gained by a power of t to approximately equalize the amplitudes in time. The magenta line is the predicted SmS arrivals after an NMO correction for the SmS. The rightmost trace in each single event receiver gather is the NMO stack.

Post-critical SmS Moho Reflections

a) shows the event locations to the south of the receiver array for event distances out to 200 km. b) displays a composite record section for the post-critical SmS arrival. This includes several event gathers recorded by the left north-south linear array stations for the transverse component. The direct S arrivals for each event gather are denoted by red arrows. The magenta dashed lines and the black arrows show the predicted SmS arrival on the composite record section.

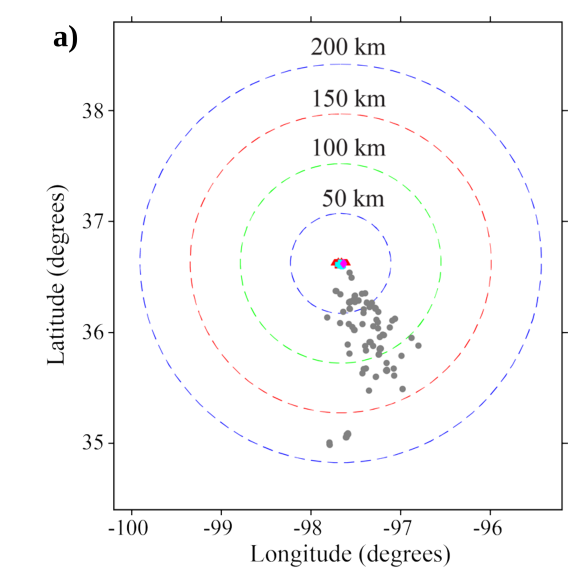

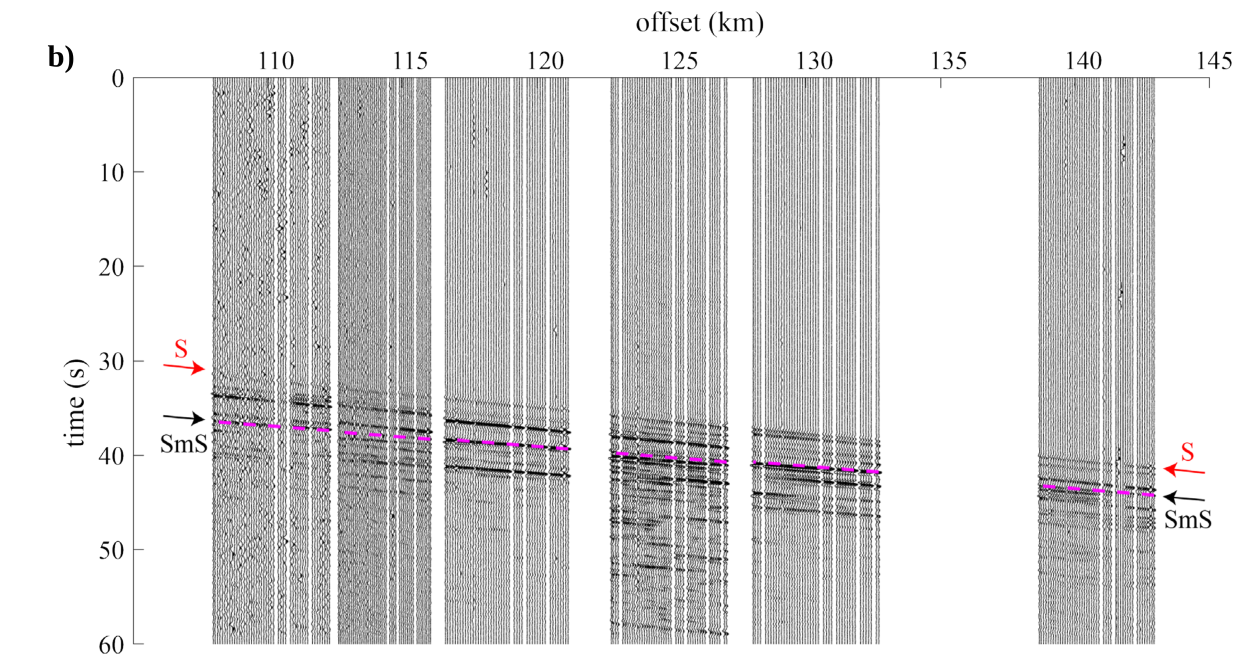

Near Offset Event Gathers for the PmP and SmS before and after Event Static Corrections

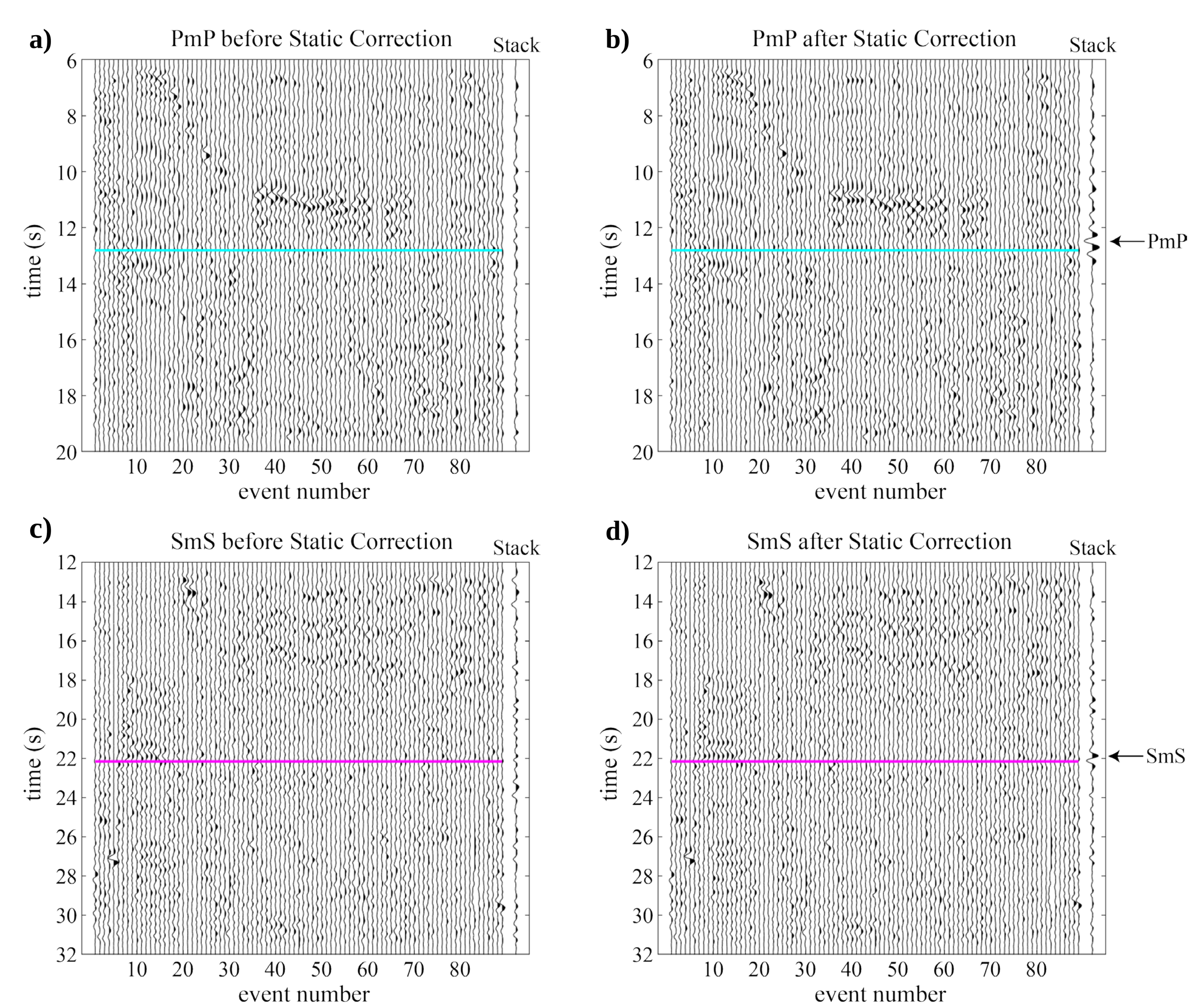

a) Vertical component event gather before event static corrections, where each trace is the stacked result for a single event on E-W linear array nodal stations. The cyan line predicts the NMO corrected PmP arrival. The rightmost trace is the event stack. b) Vertical component event gather after static corrections. Each trace on a) is cross correlated with the stacked trace to obtain the static corrections. The rightmost trace in b) is the stacked result after NMO and static corrections. c) and d) are similar results for the transverse component event gathers. The magenta lines predict the NMO and NMO plus static corrected SmS arrivals.

The OGS Catalog Event Depths and Their Uncertainties, and Deviations from the Event Static Corrections

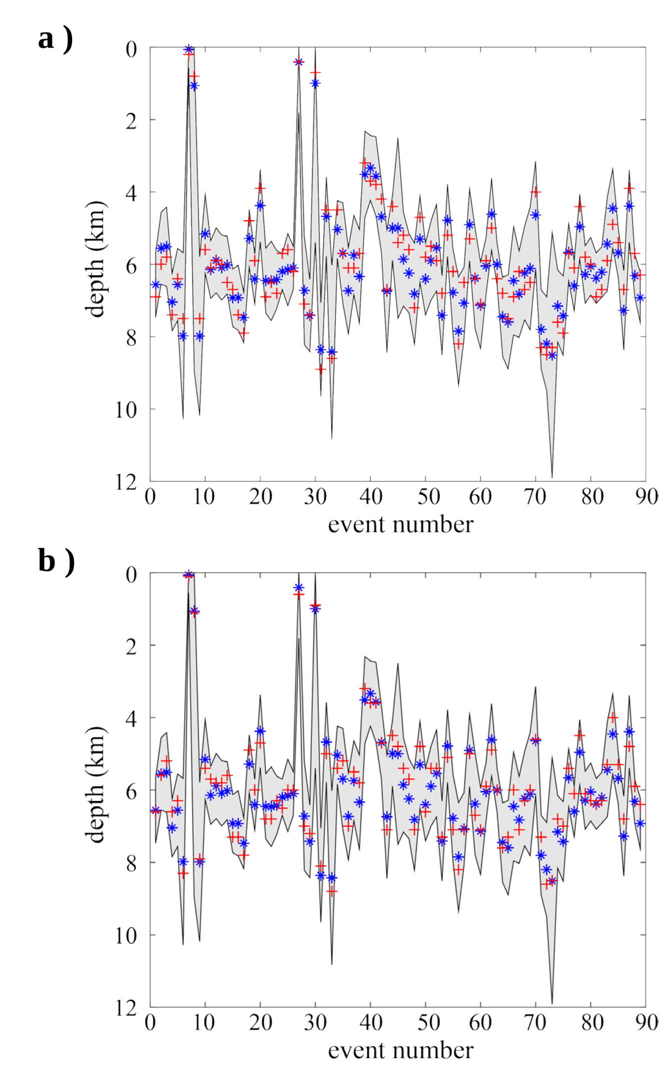

a) shows the OGS catalog event depths (blue asterisks) and their uncertainties (gray area). The red plus signs show deviations obtained from the static corrections for the PmP arrivals, and these deviations are within the depth uncertainties of the OGS catalog. However, the static corrections could also result from lateral changes in velocity. b) shows a similar plot for the SmS arrivals.

CONCLUSIONS

Preliminary conclusions of this study include:

- Near offset Moho reflections of PmP and SmS are enhanced on single event stacks through NMO corrections, low pass filtering and gaining methods.
- The stacking results of multiple near offset events show weak Moho reflections resulting from depth uncertainties and near source velocity variations.
- Event static corrections are used to enhance the near offset Moho reflection signals. The NMO stacked times of PmP and SmS arrivals are used to estimate the average Poisson's ratio (0.258), with a Vp/Vs ratio of approximately 1.75.
- The depth deviations obtained from the static corrections are within the depth uncertainties of the OGS catalog. However, the static corrections could result from lateral changes in velocity as well.
- The Moho reflections are strong on the composite record section for the post-critical SmS arrivals. This shows that the velocity model has the ability to predict the wide-angle Moho reflection signals correctly.

REFERENCES

Darold, A. P., et al. "Oklahoma earthquake summary report 2014." Okla. Geol. Surv. Open-File Rept. OF1-2015 (2015): 1-46.
Sweet, J. R., et al. "A community experiment to record the full seismic wavefield in Oklahoma." Seismological Research Letters 89.5 (2018): 1923-1930.

ACKNOWLEDGMENTS

The first author thanks the Geodata Science Program at Purdue University. This work was partially supported by NSF EAR-1839322 and a Purdue EAPS travel grant.